J Shoulder Elbow Surg (2021) 30, 544–553

ELSEVIER

Journal of Shoulder and Elbow Surgery

www.elsevier.com/locate/ymse

# Effect of kartogenin-loaded gelatin methacryloyl hydrogel scaffold with bone marrow stimulation for enthesis healing in rotator cuff repair

**Chenglong Huang, MD[a,b], Xuancheng Zhang, MD[c], Huanhuan Luo, MD[b], Jieen Pan, MD[b], Wenguo Cui, PhD[d], Biao Cheng, MD[a,*], Song Zhao, MD, PhD[c,*], Gang Chen, MD[b,*]**

[a]*Department of Orthopedics, Clinical Medical School, The Affiliated Shanghai No. 10 People's Hospital, Nanjing Medical University, Shanghai, China*
[b]*Department of Orthopaedics, The Second Affiliated Hospital of Jiaxing University, Jiaxing, Zhejiang, China*
[c]*Department of Sports Medicine, Shanghai Jiao Tong University Affiliated Sixth People's Hospital, Shanghai, China*
[d]*Shanghai Institute of Traumatology and Orthopaedics, Ruijin Hospital, Shanghai Jiaotong University School of Medicine, Shanghai, China*

**Background:** Strategies involving microfracture, biomaterials, growth factors, and chemical agents have been evaluated for improving enthesis healing. Kartogenin (KGN) promotes selective differentiation of bone marrow mesenchymal stem cells (BMSCs) into chondrocytes. Gelatin methacryloyl (GelMA) is a promising biomaterial for engineering scaffolds and drug carriers. Herein, we investigated KGN-loaded GelMA hydrogel scaffolds with a bone marrow–stimulating technique for the repair of rotator cuff tear.
**Methods:** KGN-loaded GelMA hydrogel scaffolds were obtained by ultraviolet GelMA crosslinking and vacuum freeze-drying. Fifty-four New Zealand rabbits were randomly divided into (1) repair only (control), (2) microfracture + repair (BMS), and (3) microfracture + repair augmentation with a KGN-loaded GelMA hydrogel scaffold (combined) groups. Tendons were repaired by transosseous sutures. The structure, degradation, and in vitro KGN release of the scaffolds were characterized. Animals were euthanized 4, 8, and 12 weeks after repair. Enthesis healing was evaluated by macroscopy, microcomputed tomography, histology, and biomechanical tests.
**Results:** The KGN-loaded GelMA hydrogel scaffolds are porous with a 60.4 ± 28.2-μm average pore size, and they degrade quickly in 2.5 units/mL collagenase solution. Nearly 81% of KGN was released into phosphate-buffered saline within 12 hours, whereas the remaining KGN was released in 7 days. Macroscopically, the repaired tendons were attached to the footprint. No differences were detected postoperatively in microcomputed tomography analysis among groups. Fibrous scar tissue was the main component at the tendon-to-bone interface in the control group. Disorderly arranged cartilage formation was observed at the tendon-to-bone interface in the BMS and combined groups 4 weeks after repair; the combined group exhibited relatively more cartilage. The combined

The animal experiment in this study was approved by the Animal Care and Use Committee of Jiaxing University (JUMC2019-048).

*Reprint requests: Biao Cheng, MD, Department of Orthopedics, Clinical Medical School, The Affiliated Shanghai No. 10 People's Hospital, Nanjing Medical University, Shanghai, China; Song Zhao, MD PhD, Department of Sports Medicine, Shanghai Jiao Tong University Affiliated Sixth People's Hospital, Shanghai, China; Gang Chen, MD, Department of Orthopaedics, The Second Affiliated Hospital of Jiaxing University, Jiaxing, Zhejiang, China.

E-mail addresses: chengbiaotgyx@163.com (B. Cheng); drzhaosong1980@163.com (S. Zhao); chengangtgyx@163.com (G. Chen).


https://doi.org/10.1016/j.jse.2020.06.013

group showed improved cartilage regeneration 8 and 12 weeks after repair. Similar results were found in tendon maturation scores. The ultimate load to failure and stiffness of the repaired tendon increased in all 3 groups. At 4 weeks after repair, the BMS and combined groups exhibited greater ultimate load to failure than the control group, although there was no difference in stiffness among groups. The BMS and combined groups exhibited greater ultimate load to failure and stiffness than the control group, and the combined group exhibited better values than the BMS group at 8 and 12 weeks after repair.

**Conclusion:** Compared with the bone marrow–stimulating technique, the KGN-loaded GelMA hydrogel scaffold with bone marrow stimulation improved enthesis healing by promoting fibrocartilage formation and improving the mechanical properties.

**Level of evidence:** Basic Science Study; Histology and Biomechanics; Animal Model



**Keywords:** Rotator cuff; hydrogel; bone marrow stimulation; kartogenin; enthesis; gelatin methacryloyl

The rotator cuff (RC) is vulnerable to degenerative changes relevant to its relative avascularity. RC tears have a prevalence of 23% in asymptomatic shoulders in patients >50 years of age, and the percentage increases with increasing patient age.[24] Despite the development of surgical techniques in recent years, the retear rate remains high, ranging between 14% and 43%.[9] Healthy tendon-to-bone integration includes a specialized tissue interface named the enthesis, which is a structural and compositional transition between tendon and bone. RC healing occurs through fibrovascular scar tissue formation, and the resulting neofibrovascular tissue lacks the gradient mineral distribution and continuity of collagen fibers and, hence, is mechanically weaker than the original enthesis, leading to possible retearing.[14] This absence of regenerative capacity has led to the need for new approaches to induce the functional integration process and regenerate the enthesis.

Several biologic strategies, such as growth factors, biomaterials, scaffold design, mechanical stimulation, and gene and cell therapy, have been recently introduced and tested, and these strategies can augment healing of the tendon-to-bone interface.[3] Mesenchymal stem cells (MSCs) derived from tendons, synovial tissue, adipose tissue, and bone marrow play a potential role in tendon healing.[27] Some studies have focused on the beneficial effects of bleeding of the greater tuberosity during RC repair because bone marrow mesenchymal stem cells (BMSCs) and growth factors might be potentially supplied from the bleeding surfaces to the repair site.[1,20] Recently, the bone marrow–stimulating technique, described as ''microfracture'' of the greater tuberosity, has promoted enthesis healing of the RC and decreased the retear rate.[15] Microfracture induces bleeding, fibrin clot formation, and BMSCs migrating into the fibrin clot and improving the renovation of the repair tissue. It becomes the first-line option for cartilage lesions for its wide availability, simplicity of execution, minimal invasiveness, and lower cost.[2] Results from both animal and clinical studies have demonstrated the efficacy of bone marrow stimulation technique.[18,26] Combination of bone marrow stimulation technique with an augmenting patch showed promising effects on reducing retear and mechanical failure rates in the arthroscopic repair of massive RC tears.[26] Thus, combination of bone marrow stimulation technique with a tissue engineering strategy may be a practical method to enhance enthesis healing. Because of the transitional multilayer structure of the enthesis, it is challenging for biologists and engineers to provide suitable biological and physicochemical environments that promote such unique structural formation. Bone marrow stimulation and tissue engineering scaffolds with or without cell have been suggested to facilitate cartilage regeneration.[17] An ideal approach to generate a transitional enthesis may be a biomimetic scaffold design with autologous MSCs stimulated with a combination of bioactive agents that conduct cell differentiation and extracellular matrix production. Kartogenin (KGN) is a recently identified small molecule that promotes chondrocyte differentiation. In a mouse model of osteoarthritis, intra-articular injection of KGN was demonstrated to reduce tibial plateau cartilage degeneration.[11] However, without a carrier, cartilage-like tissue is formed in the soft tissue by KGN injection as a result of leakage of KGN solution, whereas a scaffold served as a ''retainer'' of the KGN solution, preventing its diffusion into the surrounding tissues.[29] Gelatin methacryloyl (GelMA) is a versatile biomaterial with tunable physicochemical properties and remarkable compatibility for a broad spectrum of applications. GelMA-based hydrogels are biocompatible, biodegradable, noncytotoxic, and nonimmunogenic[28] and are suitable as scaffolds.

In this study, a KGN-loaded GelMA hydrogel scaffold was prepared by ultraviolet (UV) crosslinking and vacuum freeze-drying. Together with the bone marrow stimulation technique, this scaffold might serve as a promising candidate for in situ inductive enthesis regeneration without the need to employ any extraneous cells and growth factors. By establishing an acute RC tear model combined with macroscopy, microcomputed tomography, histology, and biomechanical analysis, we hypothesized that KGN-loaded GelMA hydrogel scaffolds in combination with the bone marrow stimulation technique would enhance enthesis healing.

## Materials and methods

### KGN-loaded GelMA hydrogel scaffold fabrication

Methacrylation of gelatin was performed using a previously reported method to obtain gelatin methacryloyl (GelMA).[19] Briefly, 20 g of type A gelatin (Sigma-Aldrich, St Louis, MO, USA) was mixed at 20% (w/v) into phosphate-buffered saline (PBS) at 60°C and stirred until fully dissolved. Methacrylic anhydride (16 mL; Sigma-Aldrich) was added to the gelatin solution at a rate of 0.5 mL/min under stirred conditions at 50°C and allowed to react for 1 hour. Following a 5× dilution with Dulbecco's PBS (GIBCO, Grand Island, NY, USA) to stop the reaction, the mixture was dialyzed against distilled water through 12-14-kDa cutoff dialysis tubing for 1 week at 40°C to remove the low-molecular-weight impurities. The solution was lyophilized and refrigerated until further use. The concentration of KGN was prepared as described previously.[29] Briefly, KGN (5 mg; Sigma-Aldrich) was dissolved in 0.3 mL dimethyl sulfoxide (Sigma-Aldrich) and then diluted with 2.8 mL distilled water to obtain 5 mM KGN working solutions such that each 10 μL contained 5 mM KGN. Then, KGN-loaded GelMA hydrogel was formed by mixing 10 μL KGN from the KGN- dimethyl sulfoxide solution with 0.5 mL of 5-wt% GelMA and 0.5-wt% IRGACUREVR2959 (Sigma-Aldrich). Each piece of KGN-loaded GelMA hydrogel contained 10 μL of 5 mM KGN equivalent to 100 μM of KGN-loaded GelMA hydrogel. Chemically crosslinked hydrogels were obtained by subjecting the prepolymer solutions to UV (320-500 nm) using a high-intensity UV lamp (UVSF81T; Futansi, Shanghai, China) for 90 seconds.[25] The GelMA hydrogel was incubated overnight in a refrigerator at –20°C and transferred to a vacuum freeze-drier (Virtis AdVantage; SP Industries, Gardiner, NY, USA) for 3 days to obtain a solid scaffold. All scaffolds were sterilized using $^{60}$Co irradiation for further use.

### Structural characterization of the KGN-loaded GelMA hydrogel scaffold

To observe the morphology of the KGN-loaded GelMA hydrogel scaffold, the samples were examined using a scanning electron microscope (VEGA3; TESCAN, Brno, Czech Republic). Before characterization, the samples were added directly on top of conductive tapes mounted on scanning electron microscope sample stubs and sputter-coated with gold for 60 seconds using gold sputter-coating equipment (SC7620; Quorum Technologies, Lewes, East Sussex, UK).

### Degradation of the KGN-loaded GelMA hydrogel scaffold

The in situ degradation of the scaffold in PBS and with collagenase (Sigma-Aldrich) was determined. Samples were incubated in 10 mM PBS (pH 7.4) or collagenase solution at a concentration of 2.5 units/mL in PBS at 37°C with continuous shaking. The scaffold weight loss was examined at predetermined times (on days 3, 6, 9, 12, 15, and 18 in PBS and at hours 2, 4, 6, 8, 10, 12, 14, and 16 in collagenase solution). The scaffolds were washed with distilled water, lyophilized, and weighed. Degradation was determined as the percentage weight loss according to the following equation: mass remaining (%) = $w_d/w_0 \times 100$, where $w_0$ is the original dry weight and $w_d$ is the dry weight after incubation for a certain period.[13]

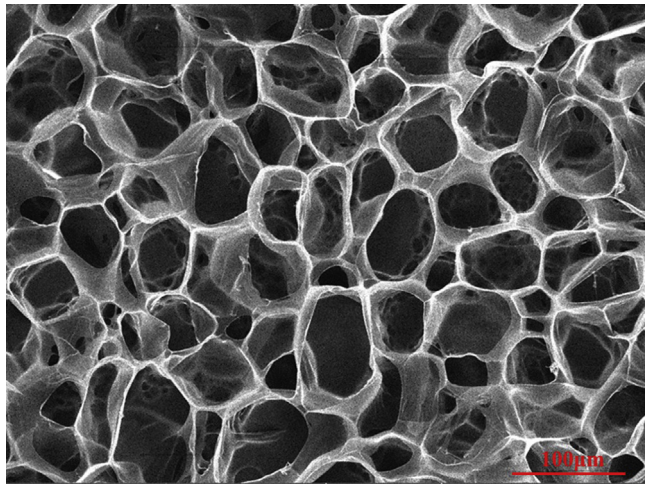


**Figure 1** Scanning electron microscope image of the KGN-loaded GelMA hydrogel scaffold. *KGN*, kartogenin; *GelMA*, gelatin methacryloyl.

### In vitro KGN release from the KGN-loaded GelMA hydrogel scaffold

Each KGN-loaded GelMA hydrogel scaffold containing 5 mM KGN was separately incubated in 15-mL tubes containing 10 mL PBS (pH 7.4) at 37°C for 7 days. PBS (0.2 mL) was collected at various time points (every 2 hours for 12 hours, followed by every 24 hours for 7 days), and the concentration of KGN was measured to estimate the amount of KGN released from the scaffold into the PBS. Another 0.2 mL of fresh PBS was supplemented to keep the PBS volume constant. KGN in PBS was quantified by high-performance liquid chromatography (Agilent 1100 HPLC system, Agilent Technologies, Santa Clara, CA, USA); the test method is described elsewhere.[30]

### Experimental design and intervention

We randomly allocated 54 adult New Zealand White female rabbits weighting 2.8-3.5 kg into 3 groups as follows: (1) repair only (control), (2) microfracture + repair (BMS), and (3) microfracture + repair augmented with KGN-loaded GelMA hydrogel scaffold (combined) groups. The animals underwent operation on either shoulder, and surgeries were performed on a randomly selected side of the shoulder. General anesthesia was carried out by intravenous injection of 3% pentobarbital sodium (1 mL/kg, intraperitoneal injection). The skin of the shoulders was shaved and sterilized with iodophor. A 2-cm longitudinal anterolateral skin incision was made, and the deltoid was split to expose the supraspinatus (SSP) tendon at its insertion. The tendon was transected at its insertion, and all fibrocartilaginous tissue attached to the footprint was removed. The footprint was decorticated lightly with a no. 15 blade knife to ensure complete debridement of the native enthesis. In the control group, tendons were repaired with transosseous sutures by 2-0 nonabsorbable sutures (polyester;

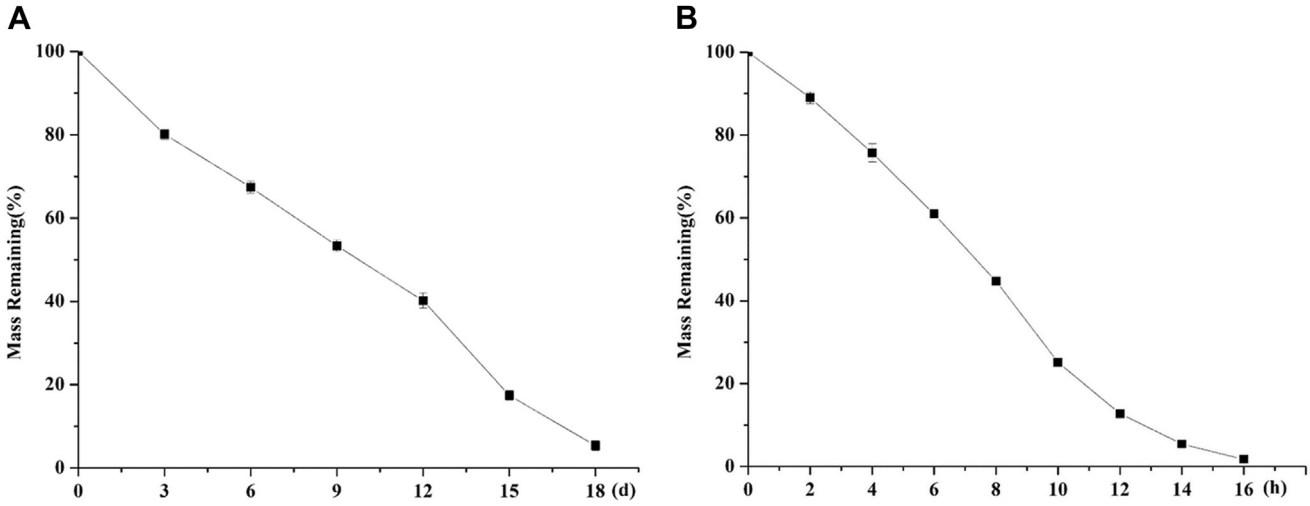


**Figure 2** (**A**) Degradation of the KGN-loaded GelMA hydrogel scaffold in phosphate-buffered saline. (**B**) Degradation of the KGN-loaded GelMA hydrogel scaffold in collagenase. *KGN*, kartogenin; *GelMA*, gelatin methacryloyl.

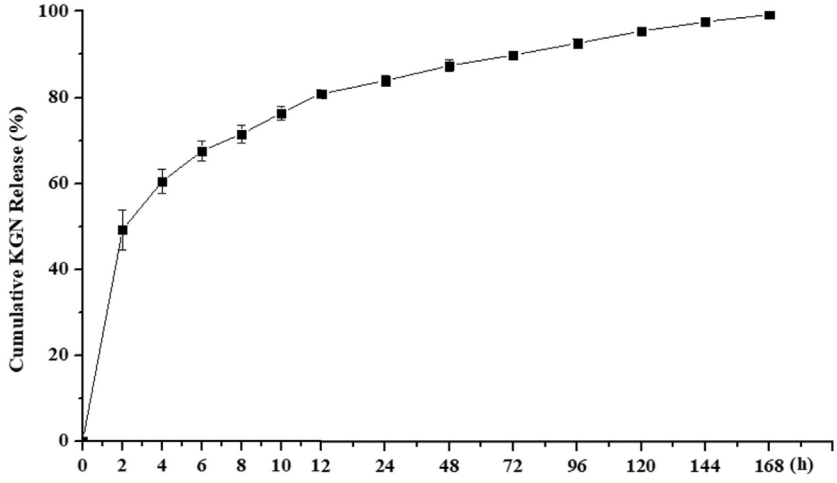


**Figure 3** In vitro KGN release of the KGN-loaded GelMA hydrogel scaffold. *KGN*, kartogenin; *GelMA*, gelatin methacryloyl.

Shanghai Pudong Jinhuan Medical Products Co., Ltd, Shanghai, China). In the BMS group, the bone marrow–stimulating technique was performed using a Kirschner wire (0.8 mm in diameter). Two holes were made 0.8 mm in diameter and 3 mm deep, and another 2 parallel bone tunnels were created from the decorticated site to the lateral aspect of the greater tuberosity. In the combined group, the bone marrow–stimulating technique was performed first, and then the scaffold, which was 2.5 mm in length, 2 mm in width, and 1 mm in thickness, was placed between the footprint and the tendon. The footprint scaffold construct made contact with the fixed tendon. The deltoid muscle and the skin were then closed with 4-0 absorbable interrupted sutures (PGA; Shanghai Pudong Jinhuan Medical Products Co., Ltd, Shanghai, China). The rabbits were allowed to exercise as desired in their respective cages with free access to water and food. All surgeries were performed by the same surgeon.

The animals were killed by intracardiac injection of a high dose of ketamine hydrochloride and xylazine hydrochloride 4, 8, and 12 weeks after the repair procedure. Eighteen animals were killed at each time point after repair. At the time of killing, the entire humeri with their SSP tendons were harvested after all other periarticular soft tissues were removed.

## Gross evaluation

Samples were macroscopically evaluated at the time of euthanasia to assess enthesis healing.

## Microcomputed tomography analysis

The SSP tendon and proximal humeral epiphysis were fixed in 4% paraformaldehyde and then assessed with micro-CT (eXplore Locus SP; GE Healthcare, London, Ontario, Canada) using the conditions of 80 kV, 450 mA, and a 0.045 mm effective pixel size.

**Table I** Results of microcomputed tomography analysis

| Group | BMD (mg/cm$^3$) | | | TMD (mg/cm$^3$) | | | BV/TV | | |
|---|---|---|---|---|---|---|---|---|---|
| | 4 weeks | 8 weeks | 12 weeks | 4 weeks | 8 weeks | 12 weeks | 4 weeks | 8 weeks | 12 weeks |
| Control | 270.3 ± 21.7 | 284.6 ± 25.1 | 303.2 ± 22.6 | 501.9 ± 23.8 | 519.9 ± 17.9 | 539.5 ± 35.1 | 0.36 ± 0.03 | 0.37 ± 0.03 | 0.38 ± 0.03 |
| BMS | 270.8 ± 19.7 | 287.4 ± 22.1 | 295.9 ± 19.8 | 508.3 ± 11.9 | 513.0 ± 9.8 | 561.2 ± 23.3 | 0.36 ± 0.04 | 0.37 ± 0.03 | 0.38 ± 0.03 |
| Combined | 277.8 ± 21.8 | 296.7 ± 21.6 | 300.9 ± 24.2 | 514.3 ± 19.9 | 522.6 ± 10.4 | 562.8 ± 34.2 | 0.38 ± 0.04 | 0.38 ± 0.04 | 0.40 ± 0.44 |
| Statistic | | | | | | | | | |
| F | 0.24 | 0.45 | 0.17 | 0.62 | 0.83 | 1.03 | 0.53 | 0.23 | 0.68 |
| P | .79 | .64 | .85 | .55 | .45 | .38 | .60 | .80 | .52 |

*BMS*, microfracture + repair group; *BMD*, bone mineral density; *TMD*, tissue mineral density; *BV/TV*, bone volume / total volume.
Data are shown as mean ± standard deviation.

The region of interest was centered at the repaired tendon-to-bone footprint. The size of the region of interest was determined based on gross observations and measurements, which indicated that the enthesis measured approximately 5 mm wide. The tissue mineral density, bone mineral density, and bone volume fraction (bone volume / total volume) were calculated for the region of interest.

## Histologic evaluation

Formalin-fixed specimens (n = 6 shoulders per group) for each time point were used for the histologic evaluation. After fixation in 10% buffered neutral formalin for 7 days, the samples were decalcified in ethylenediaminetetraacetic acid buffered saline solution (pH 7.4; 0.25 mol/L), dehydrated by serial ethanol washes, and embedded in paraffin wax. Cross sections of 5 μm were obtained from each sample by cutting it parallel to the direction of the SSP tendon insertion. The sections were stained with hematoxylin and eosin (Sigma-Aldrich) and toluidine blue stain (Sigma-Aldrich) and were assessed under a light microscope for enthesis healing by a histologist who was familiar with enthesis histology and blinded to the treatments. According to the tendon maturing scoring system described by Ide et al,[10] we semi-quantitatively evaluated the repaired tendons and their insertion. Seven histologic parameters were considered, including cellularity, proportion of cells resembling tenocytes, proportion of cells oriented parallel, vascularity, proportion of fibers of large diameter characteristic of mature tendon fibers, proportion of fibers oriented parallel, and remodeling of tendon-to-bone insertion, to determine the maturity score for tendon insertion as well as tendon proper. They used the following criteria for scoring the insertion based on the histologic findings: score 1, the insertion had continuity without fibrous tissue or bone ingrowth; score 2, the insertion had continuity with fibrous tissue ingrowth but no fibrocartilage cells; score 3, the insertion had continuity with fibrous tissue ingrowth and fibrocartilage cells but no tidemark; and score 4, the insertion had continuity with fibrous tissue ingrowth, fibrocartilage cells, and a tidemark. The sum of the scores were recorded and compared.

## Biomechanical evaluation

The remaining 6 shoulders per group for each time point were used for mechanical tests on the day of euthanasia. The free end of the SSP tendon was sutured with a no. 5 Ethibond braided suture (Ethicon, Somerville, NJ, USA) with a locking stitch suture. The proximal humerus was fixed to a mechanical testing machine (Model 5965; Instron, Norwood, MA, USA) with a custom-made clamp, and the SSP insertion site was tied to the other side of the mechanical testing machine along its native anatomic direction to form a right angle. Traction was applied along the longitudinal axis of the tendon; a preload of 0.2 N and preconditioning from 0.2 to 1 N for 10 cycles were applied to the SSP tendon to minimize soft tissue viscoelastic effects. The ultimate failure load was evaluated at 1 mm per minute, and uniaxial tension was recorded. The load-deformation curve was generated, and the ultimate load was obtained. The stiffness was defined by the slope after the toe region by the use of linear least squares regression analysis.[4]

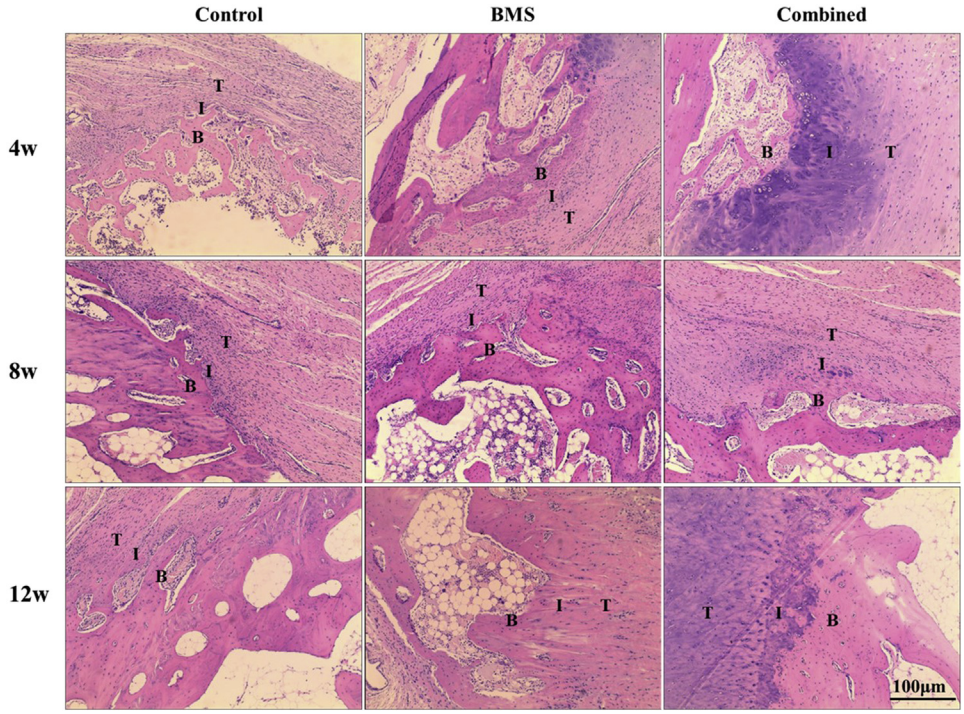


**Figure 4** Histologic evaluation of enthesis in the 3 groups at each time point after surgery. Hematoxylin and eosin staining; original magnification ×100; scale bar: 100 μm. *B*, bone; *I*, interface; *T*, tendon.

### Statistical analysis

Statistical analysis was performed using 1-way analysis of variance with post hoc testing using the Bonferroni method. The data distribution of each group was tested for normality with the Kolmogorov-Smirnov test. Continuous data are expressed as the mean ± standard deviation when the normality of the data was assessed. For all the continuous variables, differences were considered to be significant for $P$ values of $<.05$.

## Results

### Structural characterization and degradation of the KGN-loaded GelMA hydrogel scaffold

The KGN-loaded GelMA hydrogel scaffold scanning electron microscope images show that the scaffold has a porous network with an average pore size of 60.4 ± 28.2 μm (Fig. 1). It degraded slowly in PBS solution, and the degradation was approximately 48% on the 9th day and approximately 95% on the 18th day. When incubated in collagenase, the scaffold degraded quickly and was thoroughly degraded after 18 hours (Fig. 2).

### In vitro KGN release from the KGN-loaded GelMA hydrogel scaffold

To determine KGN release in vitro, we performed a 7-day release test. KGN was detected in the first 2 hours and released quickly in the first 6 hours, followed by a slow increase from 6 hours to 6 days, after which the release plateaued. Nearly 81% of the total KGN in the scaffold was released in PBS within the first 12 hours, and 7 days were needed to release the remaining KGN (Fig. 3).

### Gross evaluation

Macroscopic assessment of the samples indicated that the repaired tendons healed in all groups, and no evidence of infection was found, and the nonabsorbable suture remained in place. All the SSP tendons were attached to the footprint on the greater tuberosity, and there was no defect in any part of the enthesis. No scaffold remnant was found on the footprint in the combined group.

### Microcomputed tomography analysis

There were no significant differences in tissue mineral density, bone mineral density, and bone volume fraction among the 3 groups at any time point after repair (Table I).

### Histologic evaluation

In addition to hematoxylin and eosin staining (Fig. 4), toluidine blue staining was used for morphologic assessment of cartilage subtypes in the histologic evaluation. Cartilage was determined by metachromasia with toluidine blue staining (Fig. 5). At 4 weeks, the tendon-to-bone interface

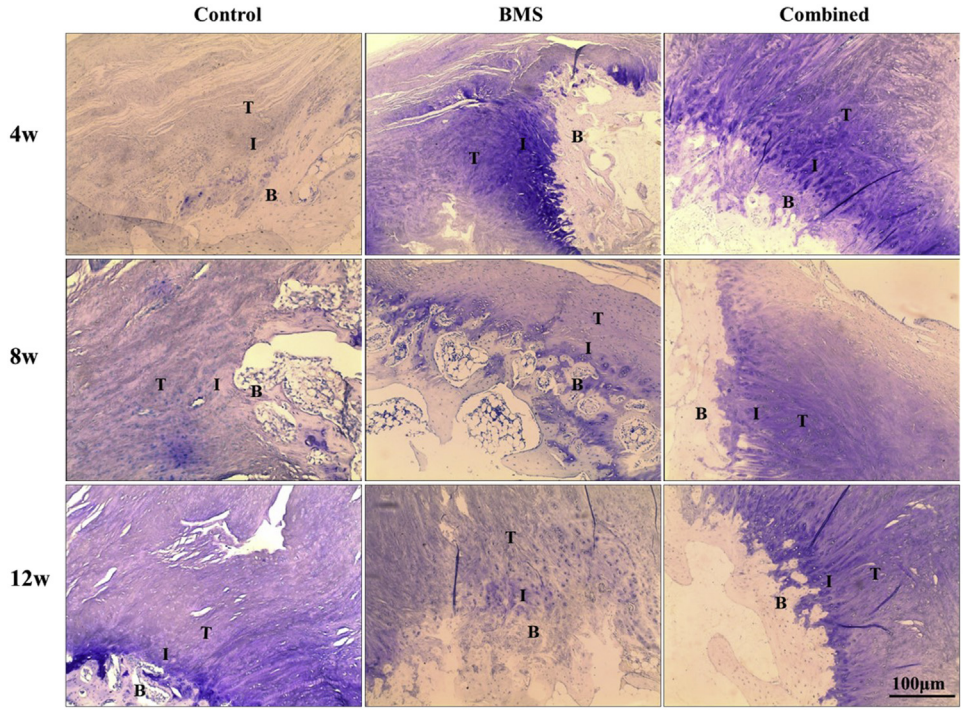


**Figure 5** Histologic evaluation of enthesis in the 3 groups at each time point after surgery. Toluidine blue staining; original magnification ×100; scale bar: 100 μm. *B*, bone; *I*, interface; *T*, tendon.

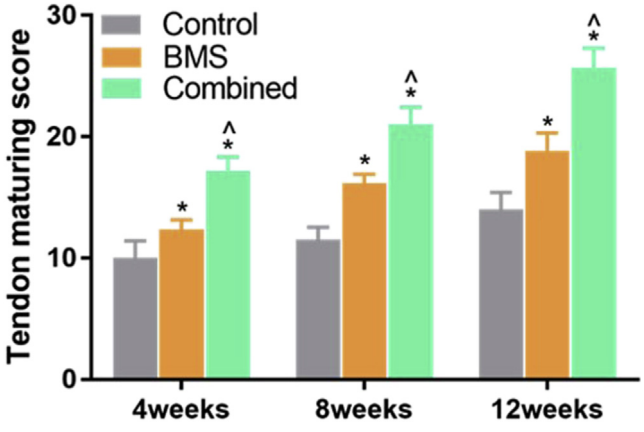


**Figure 6** Tendon maturing score of the repaired rotator cuff. Results are shown as mean ± standard deviation (*$P < .05$ vs. control; ^$P < .05$ vs. BMS). *BMS*, microfracture + repair group.

was replaced by fibrous scar tissue, and no metachromasia with toluidine blue staining was found in the control group. Disorderly arranged fibrocartilage formation was observed in the BMS group and the combined group, but more fibrocartilage formation was observed in the combined group. The scaffold in the combined group degraded completely, and no fibrovascular granular tissue was observed at the tendon-to-bone interface. At 8 weeks, fibrous scar tissue was still the main component, with little cartilage formation at the tendon-to-bone interface in the control group. Orderly arranged cartilage formation was observed in the BMS group and the combined group, although the combined group exhibited better fibrocartilage formation than the BMS group. At 12 weeks, the microscopic findings were similar to those of the 8-week samples, and improved cartilage regeneration was found in the combined group. The tendon maturation score of the BMS group and the combined group was significantly higher than that of the control group, and the combined group scored better than the BMS group ($P < .001$) (Fig. 6).

## Biomechanical evaluation

The ultimate load to failure and stiffness of the repaired tendon increased in all 3 groups. At 4 weeks after repair, the BMS group and the combined group exhibited greater ultimate load to failure than the control group ($P = .003$), whereas there was no difference in stiffness among groups ($P = .666$). The ultimate load to failure and stiffness of the BMS group and the combined group were better than those of the control group, and the combined group was better than the BMS group at 8 and 12 weeks after repair ($P < .001$) (Fig. 7).

## Discussion

This study investigated the effects of KGN-loaded GelMA hydrogel scaffolds with bone marrow stimulation on enthesis healing after RC repair in rabbits. The results of

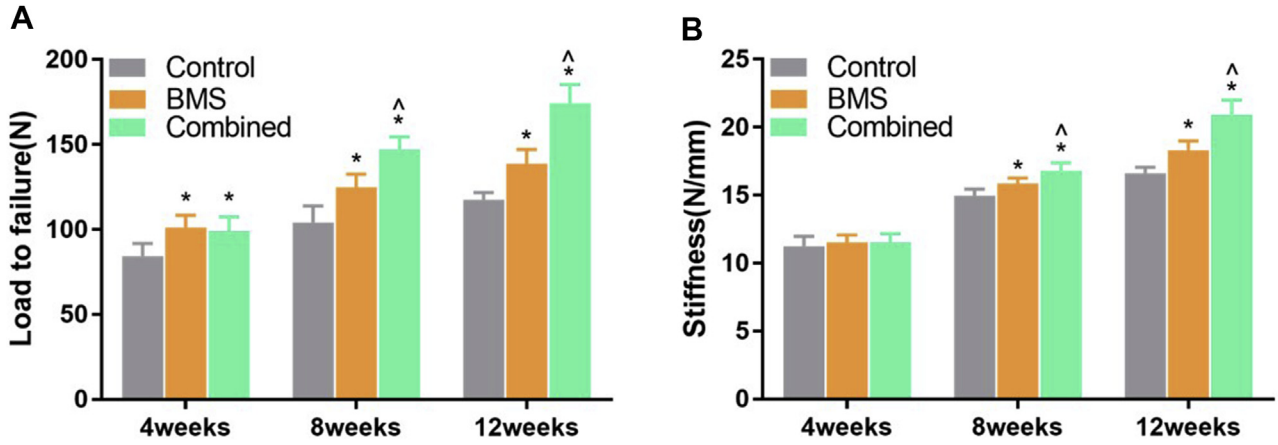


**Figure 7** Biomechanical test of the repaired rotator cuff: (**A**) ultimate load to failure; (**B**) stiffness. Results are shown as mean ± standard deviation (*$P < .05$ vs. control; ^$P < .05$ vs. BMS). *BMS*, microfracture + repair group.

this study confirmed that KGN-loaded GelMA hydrogel scaffolds with bone marrow stimulation can enhance enthesis healing and promote better outcomes than bone marrow stimulation alone.

MSCs can differentiate into various musculoskeletal tissue types, including osteoblasts, fibroblasts, and chondrocytes, and secrete bioactive molecules that provide a regenerative microenvironment.[21] However, stem cell technologies are faced with problems such as time-consuming procedures, a shortage of cell sources, uncertain regulation of stem cell differentiation, possible host immune reactions, and difficultly storing and transporting the constructs, leading to a low possibility of clinical translation.[5]

The bone marrow–stimulating technique is an efficient way to promote BMSCs. Milano et al[18] reported the efficacy of a marrow-stimulating technique with microfracture of the greater tuberosity during arthroscopic RC repair, which led to a better healing rate in the microfracture group for large tears involving the SSP and infraspinatus. Bilsel et al[1] evaluated a chronic RC tear model to investigate the effect of microfracture as a bone marrow–stimulating technique for RC healing. Biomechanical and histologic findings showed that microfractures promoted dynamic tendon healing with thicker collagen bundles and more fibrocartilage. However, a controlled laboratory study of rats indicated that the application of bone marrow–derived mesenchymal stem cells did not improve the structure, composition, or strength of the healing tendon.[6] Our biomechanical test revealed a significant increase in the ultimate failure load of the repaired tendon at each time point after applying the bone marrow–stimulating technique. The tendon maturing score after applying the bone marrow–stimulating technique at each time point after surgery was significantly higher than that in the control group. These similar outcomes indicate that the bone marrow–stimulating technique improved the healing quality of the enthesis. Snyder et al[23] hypothesized that bone marrow stimulation might favor the egress of MSCs, growth factors, and other proteins that enhance enthesis healing.

GelMA is a promising drug carrier. Serafim et al[22] evaluated GelMA-polyacrylamide hybrid hydrogels as a matrix for the controlled release of a model drug and demonstrated the possibility of tuning the release profile of the antibiotic by varying the composition of the hybrid. KGN is an effective material that promotes the selective differentiation of MSCs into chondrocytes. Zhou et al[28] used platelet-rich plasma as a carrier for KGN to avoid KGN diffusion into unwanted regions, and their findings indicate that KGN, with platelet-rich plasma as a carrier, promotes the formation of fibrocartilage zone between the tendon graft and the bone interface. Although it has been proposed that platelet-rich fibrin prolongs cytokine release over days, the clinical results indicated that platelet-rich fibrin has no benefit in improving tendon healing rates or functional outcomes, and the preparation and application of platelet-rich fibrin also resulted in a significantly increased operation time.[8]

In our study, a KGN-loaded GelMA hydrogel scaffold was fabricated to verify its effectiveness in enthesis healing. RC healing occurs in 3 stages: inflammation (0-7 days), repair (5-14 days), and remodeling (after 14 days).[7] It is essential that tissue healing and scaffold degradation are in sync. Our results indicated that the KGN-loaded GelMA hydrogel scaffold degraded within the desired time, and did not hamper enthesis healing. The histologic and biomechanical findings also demonstrated that the combined group had the best enthesis healing, as the combined group exhibited multiple advantages. First, the main component of the KGN-loaded GelMA hydrogel scaffold is gelatin, which contains many arginine–glycine–aspartic acid sequences that promote cell attachment.[16] The scaffolds restricted KGN within the treated region and controlled its release, as demonstrated

by our in vitro test. Second, the scaffold can absorb BMSCs by a bone marrow–stimulating technique during surgery and reduce BMSC loss. Third, the scaffold facilitates cell infiltration and proliferation because it has a porous structure with an average size of 60.4 ± 28.2 μm. Pores of this size are known to promote cell penetration and osteochondral formation.[12] Last, the scaffold is implanted between the tendon and bone, and it can convey stress to BMSCs aggregated in the scaffold. This kind of stress leads to the autogenous accumulation of BMSCs, which can enhance enthesis healing.[4]

Although enthesis healing was assessed by adopting an established semiquantitative scoring system, this study had several limitations. We did not perform Picrosirius Red staining of sections under a polarizing microscope to assess collagen organization or immunohistochemistry to evaluate biochemical composition at the healing enthesis. The effect of the scaffold on enthesis healing was evaluated by an acute RC tear model; hence, the conclusion is not suitable for chronic RC tear.

## Conclusions

The KGN-loaded GelMA hydrogel scaffolds with bone marrow stimulation improved enthesis healing, characterized by more fibrocartilage formation and improved mechanical properties. The scaffold could act as a bridge between the repaired tendon and bone bed and would be a suitable scaffold for the clinical enhancement of enthesis healing.

## Disclaimer

The authors, their immediate families, and any research foundations with which they are affiliated have not received any financial payments or other benefits from any commercial entity related to the subject of this article.

## References


1. Bilsel K, Yildiz F, Kapicioglu M, Uzer G, Elmadag M, Pulatkan A, et al. Efficacy of bone marrow-stimulating technique in rotator cuff repair. J Shoulder Elbow Surg 2017;26:1360-6. https://doi.org/10.1016/j.jse.2017.02.014
2. Boffa A, Previtali D, Altamura SA, Zaffagnini S, Candrian C, Filardo G. Platelet-rich plasma augmentation to microfracture provides a limited benefit for the treatment of cartilage lesions: a meta-analysis. Orthop J Sports Med 2020;8:2325967120910504. https://doi.org/10.1177/2325967120910504
3. Font Tellado S, Balmayor ER, Van Griensven M. Strategies to engineer tendon/ligament-to-bone interface: biomaterials, cells and growth factors. Adv Drug Deliv Rev 2015;94:126-40. https://doi.org/10.1016/j.addr.2015.03.004
4. Friedl G, Schmidt H, Rehak I, Kostner G, Schauenstein K, Windhager R. Undifferentiated human mesenchymal stem cells (hMSCs) are highly sensitive to mechanical strain: transcriptionally controlled early osteo-chondrogenic response in vitro. Osteoarthritis Cartilage 2007;15:1293-300. https://doi.org/10.1016/j.joca.2007.04.002
5. Girlovanu M, Susman S, Soritau O, Rus-Ciuca D, Melincovici C, Constantin AM, et al. Stem cells—biological update and cell therapy progress. Clujul Med 2015;88:265-71. https://doi.org/10.15386/cjmed-483
6. Gulotta LV, Kovacevic D, Ehteshami JR, Dagher E, Packer JD, Rodeo SA. Application of bone marrow-derived mesenchymal stem cells in a rotator cuff repair model. Am J Sports Med 2009;37:2126-33. https://doi.org/10.1177/0363546509339582
7. Gulotta LV, Rodeo SA. Growth factors for rotator cuff repair. Clin Sports Med 2009;28:13-23. https://doi.org/10.1016/j.csm.2008.09.002
8. Hurley ET, Lim Fat D, Moran CJ, Mullett H. The efficacy of platelet-rich plasma and platelet-rich fibrin in arthroscopic rotator cuff repair: a meta-analysis of randomized controlled trials. Am J Sports Med 2019;47:753-61. https://doi.org/10.1177/0363546517751397
9. Hurley ET, Maye AB, Mullett H. Arthroscopic rotator cuff repair: a systematic review of overlapping meta-analyses. JBJS Rev 2019;7:e1. https://doi.org/10.2106/JBJS.RVW.18.00027
10. Ide J, Kikukawa K, Hirose J, Iyama K, Sakamoto H, Mizuta H. Reconstruction of large rotator-cuff tears with acellular dermal matrix grafts in rats. J Shoulder Elbow Surg 2009;18:288-95. https://doi.org/10.1016/j.jse.2008.09.004
11. Johnson K, Zhu S, Tremblay MS, Payette JN, Wang J, Bouchez LC, et al. A stem cell-based approach to cartilage repair. Science 2012;336:717-21. https://doi.org/10.1126/science.1215157
12. Karageorgiou V, Kaplan D. Porosity of 3D biomaterial scaffolds and osteogenesis. Biomaterials 2005;26:5474-91. https://doi.org/10.1016/j.biomaterials.2005.02.002
13. Kilic Bektas C, Hasirci V. Mimicking corneal stroma using keratocyte-loaded photopolymerizable methacrylated gelatin hydrogels. J Tissue Eng Regen Med 2018;12:e1899-910. https://doi.org/10.1002/term.2621
14. Li X, Cheng R, Sun Z, Su W, Pan G, Zhao S, et al. Flexible bipolar nanofibrous membranes for improving gradient microstructure in tendon-to-bone healing. Acta Biomaterialia 2017;61:204-16. https://doi.org/10.1016/j.actbio.2017.07.044
15. Li Z, Zhang Y. Efficacy of bone marrow stimulation in arthroscopic repair of full thickness rotator cuff tears: a meta-analysis. J Orthop Surg Res 2019;14:36. https://doi.org/10.1186/s13018-019-1072-6
16. Liu Y, Chan-Park MB. A biomimetic hydrogel based on methacrylated dextran-graft-lysine and gelatin for 3D smooth muscle cell culture. Biomaterials 2010;31:1158-70. https://doi.org/10.1016/j.biomaterials.2009.10.040
17. Makris EA, Gomoll AH, Malizos KN, Hu JC, Athanasiou KA. Repair and tissue engineering techniques for articular cartilage. Nat Rev Rheumatol 2015;11:21-34. https://doi.org/10.1038/nrrheum.2014.157
18. Milano G, Saccomanno MF, Careri S, Taccardo G, De Vitis R, Fabbriciani C. Efficacy of marrow-stimulating technique in arthroscopic rotator cuff repair: a prospective randomized study. Arthroscopy 2013;29:802-10. https://doi.org/10.1016/j.arthro.2013.01.019
19. Nichol JW, Koshy ST, Bae H, Hwang CM, Yamanlar S, Khademhosseini A. Cell-laden microengineered gelatin methacrylate hydrogels. Biomaterials 2010;31:5536-44. https://doi.org/10.1016/j.biomaterials.2010.03.064
20. Randelli P, Margheritini F, Cabitza P, Dogliotti G, Corsi MM. Release of growth factors after arthroscopic acromioplasty. Knee Surgery Sports Traumatol Arthroscopy 2009;17:98-101. https://doi.org/10.1007/s00167-008-0653-4
21. Rothrauff BB, Tuan RS. Cellular therapy in bone-tendon interface regeneration. Organogenesis 2014;10:13-28. https://doi.org/10.4161/org.27404

22. Serafim A, Tucureanu C, Petre DG, Dragusin DM, Salageanu A, Van Vlierberghe S, et al. One-pot synthesis of superabsorbent hybrid hydrogels based on methacrylamide gelatin and polyacrylamide. Effortless control of hydrogel properties through composition design. N J Chem 2014;38:3112-26. https://doi.org/10.1039/c4nj00161c
23. Snyder SJ, Burns J. Rotator cuff healing and the bone marrow ''crimson duvet'' from clinical observations to science. Tech Shoulder Elbow Surg 2009;10:130-7. https://doi.org/10.1097/bte.0b013e3181c2a940
24. Tempelhof S, Rupp S, Seil R. Age-related prevalence of rotator cuff tears in asymptomatic shoulders. J Shoulder Elbow Surg 1999;8:296-9.
25. Thakur T, Xavier JR, Cross L, Jaiswal MK, Mondragon E, Kaunas R, et al. Photocrosslinkable and elastomeric hydrogels for bone regeneration. J Biomed Mater Res A 2016;104:879-88. https://doi.org/10.1002/jbm.a.35621
26. Yoon JP, Chung SW, Kim JY, Lee BJ, Kim HS, Kim JE, et al. Outcomes of combined bone marrow stimulation and patch augmentation for massive rotator cuff tears. Am J Sports Med 2016;44:963-71. https://doi.org/10.1177/0363546515625044
27. Youngstrom DW, LaDow JE, Barrett JG. Tenogenesis of bone marrow-, adipose-, and tendon-derived stem cells in a dynamic bioreactor. Connect Tissue Res 2016;57:454-65. https://doi.org/10.3109/03008207.2015.1117458
28. Yue K, Trujillo-de Santiago G, Alvarez MM, Tamayol A, Annabi N, Khademhosseini A. Synthesis, properties, and biomedical applications of gelatin methacryloyl (GelMA) hydrogels. Biomaterials 2015;73:254-71. https://doi.org/10.1016/j.biomaterials.2015.08.045
29. Zhang J, Yuan T, Zheng N, Zhou Y, Hogan MV, Wang JH. The combined use of kartogenin and platelet-rich plasma promotes fibrocartilage formation in the wounded rat Achilles tendon entheses. Bone Joint Res 2017;6:231-44. https://doi.org/10.1302/2046-3758.64.BJR-2017-0268.R1
30. Zhou Y, Zhang J, Yang J, Narava M, Zhao G, Yuan T, et al. Kartogenin with PRP promotes the formation of fibrocartilage zone in the tendon-bone interface. J Tissue Eng Regen Med 2017;11:3445-56. https://doi.org/10.1002/term.2258